330
GEOME 2
Manuscript received: December 4, 2017
Accepted: December 16, 2017

Geologica Macedonica, Vol**. 31**, No. 2, pp. 157–170 (2017)
In print: ISSN 0352 – 1206
On line: ISSN 1857 – 8586
UDC: 539.16:551.510.411]:546.296
Original scientific paper

PARAMETERS INFLUENCING DEVIATION OF RADON CONCENTRATION FROM ITS TYPICAL DIURNAL PATTERN IN THE WINTER AND SUMMER SEASONS

Dafina Kikaj[1], Janja Vaupotič[2]

[1]*Jožef Stefan International Postgraduate School, Jamova cesta 39, 1000 Ljubljana, Slovenia*
[2]*Jožef Stefan Institute, Department of Environmental Sciences, Jamova cesta 39, 1000 Ljubljana, Slovenia*
dafina.kikaj@ijs.si

A b s t r a c t: Radon (^{222}Rn) has been used as an atmospheric tracer for studying the vertical mixing processes in the planetary boundary layer (PBL). Therefore, the time series of hourly atmospheric radon concentration obtained in Ljubljana city were analyzed along with the meteorological data and back trajectory information from December 2016 to November 2017. Radon concentration exhibited the annual cycle with a higher mean in the winter (20.7 ± 15.5 Bq m^{-3}) and a lower mean in the summer (14.6 ± 9 Bq m^{-3}) reflecting the PBL evolution on a seasonal timescale. Most of the time, radon showed the typical diurnal variation following its related mean seasonal level attributed to the vertical mixing processes. Among this typical pattern, deviations of atmospheric radon concentration by more than $\pm\sigma$ from the related seasonal mean value have been detected in 9 events ($\pm\sigma$ E_i) in the winter and summer seasons using simple statistical analysis. The parameter persistent/nocturnal inversion has usually been the reason for $+\sigma$ E_i. While, the temporal variation of the exhalation rate, wind direction/speed and maritime air masses have been the responsible influencing parameter for $-\sigma$ E_i.

Key words: atmospheric radon; continuous measurement; deviations in concentration; planetary boundary layer; persistent inversion; air masses

1. INTRODUCTION

Radon (^{222}Rn) is a radioactive noble gas appearing naturally in the environment as a product of radioactive transformation of radium (^{226}Ra). Only a fraction of radon atoms is able to emanate from the mineral grains and enter into air-filled pore space, transport through these pore space by diffusion and, for a longer distance, by advection, dissolved either in water or in carrier gases (Nazaroff, 1992). Eventually, it exhales into the atmosphere where it is distributed by turbulent mixing. The exhalation of radon into the atmosphere depends on many parameters, including its source (^{226}Ra content in the soil), geology (lithology), physical characteristics of upper soil layer (mineral structure, porosity, water content) and the combination of meteorological parameters (mainly of soil moisture, atmospheric pressure gradient and temperature) (Etiope & Martinelli, 2002; Levin et al., 2002; Mazur & Kozak, 2014; Papachristodoulou et al., 2007).

Much of the early interest in radon monitoring was related to the recognition of radon as a health risk in dwellings and working environments (WHO, 2009). Atmospheric levels of radon are typically more than an order of magnitude lower than generally obtained in dwellings and the working environment (Burian & Otahal, 2009; Sesana et al., 2003; Vaupotič et al., 2010). The keen interest in atmospheric radon monitoring can be attributed to its unique characteristics as a tracer for atmospheric processes. As a gas, it is mobile and carries information over long distances across Earth's crust, oceans and atmosphere. Being noble, its mobility is not affected by chemical reactions with any medium it passes. Furthermore, since radon is relatively insoluble in water, it is not susceptible to dry or wet atmospheric removal processes. The half-life of radon (3.82 d) is comparable to the lifetimes of the short-lived atmospheric pollutants (e.g. NO_x, SO_2, CO, O_3) and atmospheric residence time of water

and aerosols. Since its half-life is much larger than turbulent timescales (< 1 h), it can be considered a fairly conservative tracer for convective boundary layer (CBL) and nocturnal boundary layer (NBL) mixing studies. With a few assumptions, it is possible to derive an "equivalent mixing height" from a time series of near ground radon concentration for a selected time period of the diurnal cycle. The equivalent mixing height is derived from a box model of the accumulation of radon at night and then its dilution the following morning (Fontan et al., 1979; Sesana et al., 2003, 2006; Griffiths et al., 2013). Since terrestrial radon exhalation is 2–3 orders of magnitude greater than its oceanic exhalation, there is a large contrast in continental and oceanic air masses radon concentration. Radon's only significant atmospheric sink is radioactive decay process.

The first atmospheric radon observations sought to characterize the vertical distribution of radon in the atmosphere (Butterweck et al., 1994; Cohen et al., 1972; Moses et al., 1960; Ussler et al., 1994). The application of radon observations from the network of available ground stations has increased substantially over the last two decades (Zahorowski et al., 2004). Nowadays, 41 stations worldwide are identified where atmospheric radon is measured regularly for periods longer than one year (Zhang et al., 2011).

Currently, there are four major applications of radon in climate, air quality and pollution studies: 1) Tracing of horizontal air mass transport (Chambers et al., 2013; Dörr et al., 1983; Zahorowski et al., 2005) (C5). 2) Investigating vertical mixing in the lower atmosphere (Chambers et al., 2014; Grossi et al., 2016; Vinuesa et al., 2007; Williams et al., 2011). 3) Assessing the surface emissions of major greenhouse gases, such as CO_2, N_2O and CH_4 (Levin et al., 1999; Van der Laan et al., 2014; Vogel et al., 2012; Wada et al., 2013); 4) Validating and, to a lesser extent, parameterising, transport and mixing schemes in climate/weather models (Jacob & Prather, 1990).

A typical pattern of atmospheric radon on the simplest of cases has been documented most of the time, such as reaching a minimum during the CBL (on cloud-free day) when the vertical dilution occurs by combined thermal circulations and mechanical mixing and a maximum concentration during the night (NBL in near-neutral to moderately stable conditions) due to the formation of a surface temperature inversion. In the very stable boundary layer (persistent and strong nocturnal inversion) and in coupled cloud layers, vertical mixing processes remain poorly understood (Chambers et al., 2011, 2015; Chen et al., 2016; Willimas et al., 2011).

Among the typical pattern of atmospheric radon on the diurnal timescale attributed to the vertical mixing processes, sudden changes (either increase or decrease from the related mean seasonal value, here in after referred to as "events") may be observed in the time series of atmospheric radon. The objective of our work was the identification of the events in the winter and summer seasons and their relation to the parameters influencing deviation of radon concentration (i) persistent and strong nocturnal inversion, (ii) temporal variability of exhalation rate, (iii) wind direction/speed and (iv) history of air masses.

2. SITE AND METHODS

2.1. *Site characteristics*

All the observations were made at the meteorological station Ljubljana Bežigrad (46°07' N, 14°52' E), situated in the central part of the city. The city of Ljubljana is located between the "Ljubljansko polje" (Ljubljana Basin) in the north, bounded by hills, north by Šmarna Gora and Rašica hills that connect Polhov Gradec hills in the west with Posavje hills in the east. To the south is "Ljubjansko barje" (Ljubljana moor, 162 km^2) (Šajn et al., 2011), a drained ancient moor that was frequently a lake during the ice ages (Pak, 1992). Ljubljana Basin lies in a very clear-cut valley basin with a relief energy of about 300 m.

Temperate and continental, the city's climate can be classified as being typical for south-Alpine regions. Characteristics features of the local climate are generally calm winds within the basin results in a high amount of foggy days, frequent persistent and strong nocturnal inversion at 350 m altitude (120 d y^{-1}), especially in the winter. The prevailing winds are NE, NNE and ENE (ARSO, 2017). The mean wind speed was 1.3 m s^{-1} during the winter and 1.4 m s^{-1} during the summer. The mean air temperature at the site reveals a distinct seasonal cycle, with the summer mean daily maximum reaching 22°C and the winter mean daily minimum 0°C. Rainfall distribution is irregular, with a peak in the summer (ARSO, 2017).

Ljubljana Basin is located in a shallow sedimentary basin filled with heterogeneous Quaternary deposits. The bedrock of the basin is built of Permian and Carboniferous clastic rocks (claystones, sandstones, conglomerates) and partly of Mesozoic carbonate rocks. It outcrops on the margins of the hills. Ljubljana Basin is covered by gravel deposits of the Sava river and by sea and lake sediments. On the gravelly Ljubljana Basin, most water goes underground (Gregorič et al., 2013).

2.2. *Measurements method*

Continuous radon monitoring has been conducted by an AlphaGuard monitor (Saphymo, Germany), ionisation chamber operating in diffusion mode with a 1-h integration time, with a lower limit of detection (LLD) ~ 2 Bq m^{-3}. The device was set up inside the weather instrument shelter (Figure 1), 1.5 m above the ground. In addition to the radon measurements, hourly values of air temperature, relative humidity, wind speed, wind direction, wind gust, atmospheric pressure, precipitation, cloud cover, solar energy radiation and diffusive energy radiation were obtained from the Office of Meteorology of the Environmental Agency of the Republic of Slovenia. Backward trajectory analysis has been performed by using HYSPLIT (Hybrid Single Particle Lagrangian Integrated Trajectory) model (Draxler and Rolph, 2011) supplied by NOAA/ARL (National Oceanic and Atmospheric Administration/Air Resources Laboratory).

Fig 1. The weather instrument shelter with the AlphaGuard monitor inside at the meteorological station Ljubljana Bežigrad located at the Environmental Agency of the Republic of Slovenia

The grid resolution has been set to 1°× 1°. Mixing layer heights were used to assist the interpretation of the atmospheric data generated by the global data assimilation system (GDAS) model from NOAA/ARL (National Oceanic and Atmospheric Administration/Air Resources Laboratory).

The statistical analyses were performed by the openair package (Carslaw & Ropkins, 2012) under R 3.3.1 (R Development Core Team, 2008).

All reported times are local times (LST = UTC + 1 h) and the northern hemisphere seasonal convection has been adapted (i.e. Winter: December–February; Spring: March–May; Summer: June –August; Autumn: September–November).

2.3. *Methodology of data analysis*

The time series of hourly mean concentrations of atmospheric radon obtained between December 2016 and November 2017 (Figure 2) was split into four seasons, as described hereinabove. For this study, the means of atmospheric radon concentration were calculated separately for the winter and summer seasons. Atmospheric radon events were first expressed as deviations in a radon concentration of more than ±σ from the mean seasonal value. Secondly, to improve the identification of events, we chose the periods when:

1. radon concentration deviates by more than +σ from the releated mean seasonal value for more than 24 hours; they are considered as events caused possibly by persistent inversion or history of air masses;
2. radon concentration deviates by more than –σ from the releated mean seasonal value for more than 24 hours; they are considered as events caused possibly by temporal variability of exhalation rate, wind direction/speed or history of air masses.

The 24 hour period has been selected to represent: (i) the synoptic timescales (days to weeks) (i)

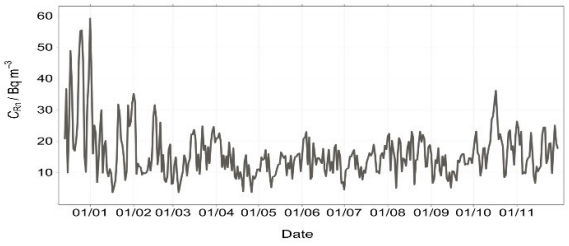

Fig. 2. Time series of daily mean atmospheric radon concentration in the period December 2016 – November 2017

persistent inversion which extends over few days and (iii) temporal variations of constant exhalation rate of radon associated mainly with water content of the soil (which implies the frequency and amount of precipitation). The frontal situations with the fast changes of gradient atmospheric pressure were not considered in this study.

To identify the strong nocturnal boundary layer (strong inversion), which breaks up near the afternoon, the condition when radon concentration deviates by more than +σ from the related seasonal value for more than 12 hours is considered as events possibly caused by strong nocturnal inversion.

3. RESULTS AND DISCUSSION

Hourly atmospheric radon concentration in the winter and summer as well as air temperature, solar energy radiation, diffusive energy radiation, atmospheric pressure, precipitation, mixing height are shown in Figures 3 and 4. Radon concentration exhibited the annual cycle with higher mean in the winter (20.7 ± 15.5 Bq m^{-3}) and lower mean in the summer (14.6 ± 9 Bq m^{-3}) reflecting the planetary boundary layer (PBL) evolution. During the winter, more cooling occurs during the long nights than heating during the short day, in the fair weather over land, reflecting the shrinking role of vertical mixing within PBL (Figure 3).

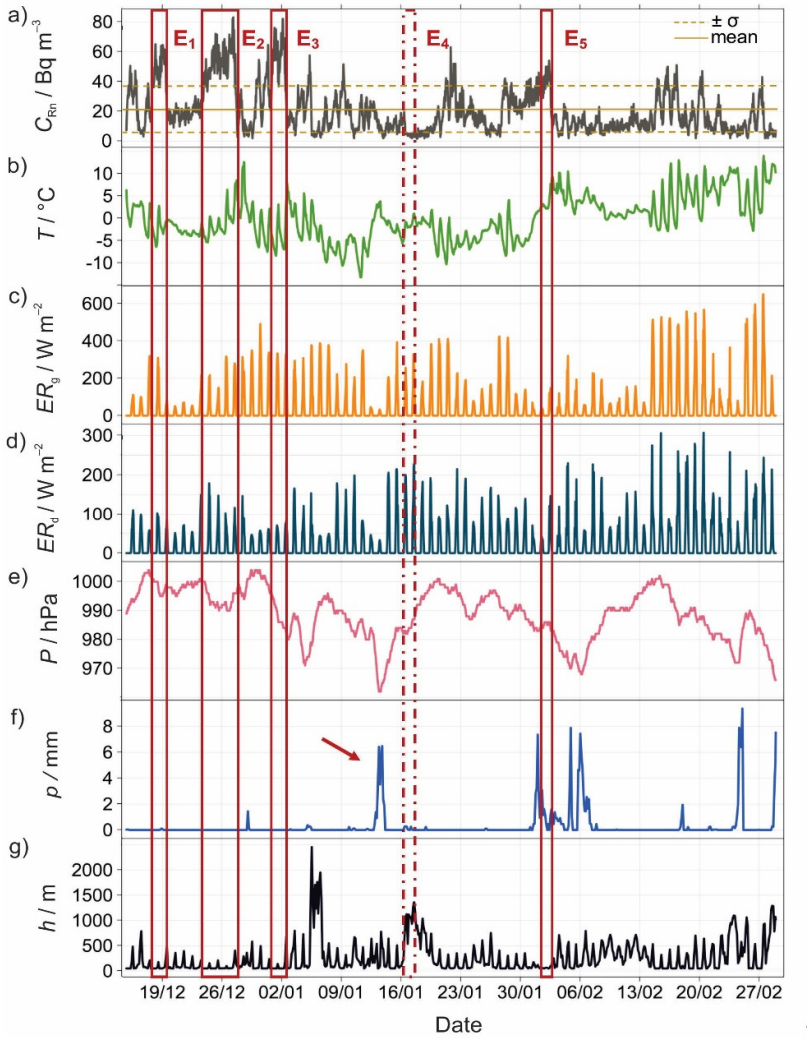

Fig. 3. Time series of a) atmospheric radon concentration (C_{Rn}), b) air temperature (T), c) global energy radiation (ER), d) diffusive energy radiation (ER), e) atmospheric pressure (P), f) precipitation (p) and g) mixing height (h) in the winter; open red boxes indicate events marked E_1, E_2, E_3, E_4 and E_5, discussed in section 3

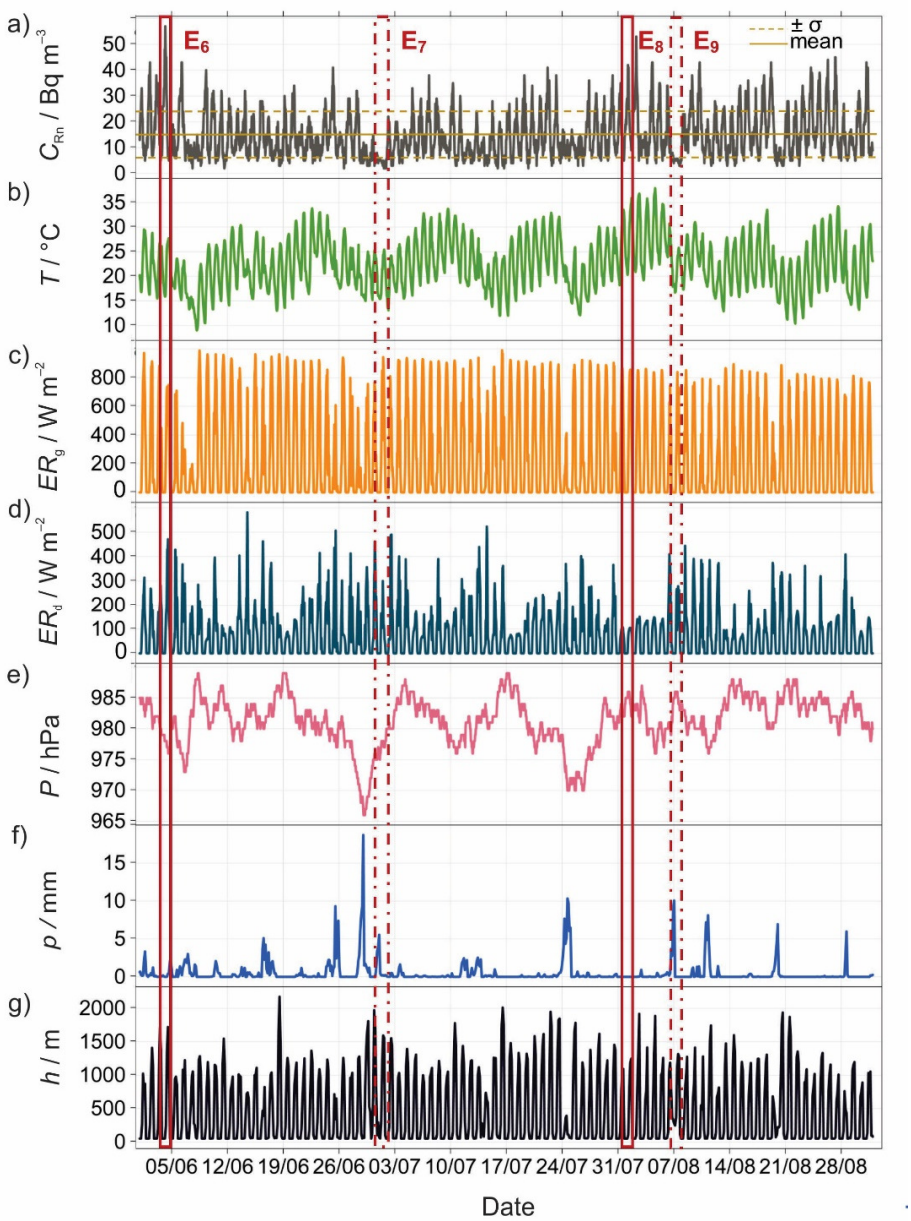

Fig. 4. Time series of a) atmospheric radon concentration (C_{Rn}), b) air temperature (T), c) global energy radiation (ER), d) diffusive energy radiation (ER), e) atmospheric pressure (P), f) precipitation (p) and g) mixing height (h) in the summer; open red boxes indicate events, marked E_6, E_7, E_8, and E_9, discussed in section 3

The growing of vertical mixing within PBL occurs during the summer, driven by the longer exposure of the land to sunlight as a result of days longer than nights (Figure 4) (Stull, 2011). Higher radon concentration in the winter and lower radon concentration in the summer was found by Pal et al., (2015) in central Europe, in southern Finland by Chen et al., (2016) and in Milan by Sesana et al., (2003).

The main distribution characteristics of atmospheric radon concentration, air temperature, relative humidity, wind speed and precipitation (mean, standard deviation, mean daily maximum and mean daily minimum) for the winter and summer seasons are shown in Table 1.

Vertical processes in very stable conditions, in mechanical turbulence (interaction of wind speed and surface roughness elements) and in cloudy days, horizontal processes and temporal variations in exhalation rate were assumed to affect the changes of radon concentration in the winter and summer for more than ±σ from the mean seasonal level for more than 24 hours. Concentrations outside of this region are considered as events and further evaluated.

Table 1

Basic statistics of radon concentration (C_{Rn}), air temperature (T), atmospheric pressure (P), relative humidity (RH), wind speed (ws) and precipitation (p) in the winter and summer seasons

	Winter December 2016–February 2017				Summer June–August 2017			
	AM	SD	AM max	AM min	AM	SD	AM max	AM min
C_{Rn} (Bq m^{-3})	20.7	15.5	35	9	14.6	9	29	5
T (°C)	–0.03	5	3	–3	22	5	29	16
P (hPa)	988	9	991	986	981	4	983	979
RH (%)	77	16	88	62	61	18	85	38
ws (m s^{-1})	1.3	1	2.6	0.4	1.5	1	3	0.2
p (mm)	0.3	1.1	1.1	0.05	0.5	1.5	2	0.03

AM – arithmetic mean, SD – standard deviation, AM max – mean daily maximum, AM min – mean daily minimum

A total of five events (hereinafter E_i) were detected in the winter 2016–17, their characteristics are reported in Table 2. Four of E_i were +σ (E_1, E_2, E_3 and E_5) and one –σ (E_4). E_5 has a short duration (14 hours) and is related to nocturnal inversion. E_1 and E_3 (duration 38 and 34 hours) are related with stable conditions (persistent inversion), and E_2 (with significantly longer duration of 75 hours) with very strong stable conditions (persistent inversion). All +σ E_i were compared with a bulk temperature gradient with a simple method for the detection of persistent inversions based on near ground temperature data on different altitudes as developed by Largeron and Staquet (2016) and a clear relation was confirmed.

Table 2

±σ E_i detected using criteria from section 2.3. The duration of each event and most responsible influencing parameter of the event.

Event	Duration	Influencing parameter
+σ E_1	18/12/2016 00:00 – 19/12/2016 10:00 (34 hours)	Persistent inversion
+σ E_2	24/12/2016 08:00 – 27/12/2016 12:00 (75 hours)	Persistent inversion
+σ E_3	31/12/2016 20:00 – 02/01/2017 10:00 (38 hours)	Nocturnal inversion
–σ E_4	16/01/2017 13:00 – 17/01/2017 23:00 (35 hours)	Katabatic wind and temporal variation of exhalation rate
+σ E_5	01/02/2017 23:00 – 02/02/2017 13:00 (14 hours)	Nocturnal inversion
+σ E_6	03/06/2017 21:00 – 04/06/2017 10:00 (13 hours)	Nocturnal inversion
–σ E_7	01/07/2017 00:00 – 02/07/2017 00:00 (24 hours)	Maritime air masses
+σ E_8	01/08/2017 22:00 – 02/08/2017 11:00 (13 hours)	Nocturnal inversion
–σ E_9	06/08/2017 23:00 – 07/08/2017 23:00 (24 hours)	Temporal variation of exhalation rate

The meteorological parameters, such as precipitation few days before (Figure 3f) and katabatic (downslope) wind with moderate speed revealed the reasons for –σ E_4.

In summer 2017, four E_i were detected. The main characteristics of each E_i in summer are presented in Table 2. Two +σ E_i (E_6 and E_8) were related to the nocturnal inversion (duration 13 hours), broke-up within 5–6 hours after sunrise. The very low level of radon concentration in the air during –σ E_7 was the result of the horizontal processes, connected to the maritime air masses, coming from the Adriatic Sea accompanied by southwestern winds.

While $-\sigma$ E_9 is explained with moderate wind speed during night and day and effect of the soil moisture on the exhalation rate of radon concentration.

The following four events, marked as E_3, E_4, E_6 and E_7, are explained in more details in the following sub chapters.

3.1. *The response of the atmospheric radon concentration to the nocturnal/persistent inversion (E_3 and E_6)*

High atmospheric pressure (> 985 hPa) under generally clear sky conditions (Figures 3e and 5f) occurred before and during E_3 (31/12/2016 20:00 – 2/01/2017 10:00). Wind speed remained below 0.5 m s^{-1}, air temperature and relative humidity showed a clear diurnal variation pattern (Figures 5b, 5d and 5e), typical for such conditions (Schnelle & Brown, 2002; Whiteman et al., 1999). There was no rainfall throughout the period.

The diurnal variation of atmospheric radon concentration with a maximum (~ 80 Bq m^{-3}) early in the morning and minimum (~ 40 Bq m^{-3}) in the afternoon was linked to the vertical mixing in the atmosphere; the mixing height was less than 300 m above ground level (a.g.l.) during daytime and as low as 50 m a.g.l. at night (Figure 3g). The mixing height evenly matched with the inversion in the basin which often fills the whole mixing layer from the ground to an inversion top which usually coincides with an average elevation of the peak surrounding the basin. In our case, this average elevation is about 695 m.

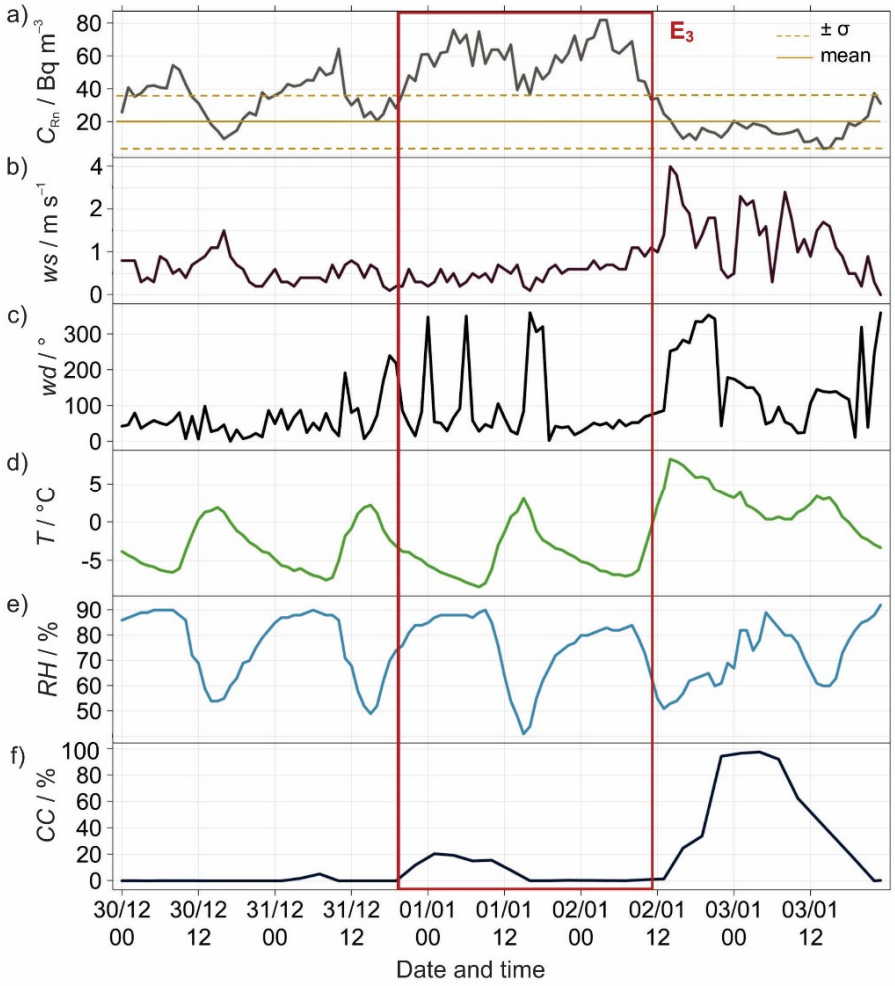

Fig. 5. Time series of a) atmospheric radon concentration (C_{Rn}), b) wind speed (*ws*), c) wind direction (*wd*), d) air temperature (*T*), e) relative humidity (*RH*) and f) cloud cover (*CC*) during the period before and after +σ E_3 (31/12/2016 20:00 – 02/01/2017 10:00)

The persistent inversion broke up within 3 hours after sunrise on 2 January (Figure 5a). The end of E_3 was with a low-pressure (< 980 hPa), enhanced wind speed (Figures 3e and 5b), which might be channelled in the basin and destroyed the persistent inversion (Whiteman et al., 2004). Radon concentration decreased rapidly achieving the typical mean level (Figure 5a).

Beginning on the morning of 3 June (E_6), the sky was clear with maximum air temperature 25°C and maximum wind speed ~ 4 m s^{-1} (Figures 6b, 6d and 6f). The atmospheric radon showed a typical diurnal variation with a minimum (7 Bq m^{-3}) in the afternoon (Figure 6a). After the sunset, the gradually built-up of radon concentration occurred with a maximum (55 Bq m^{-3}) by diverting the mean seasonal level, under the very calm wind speed conditions (Figures 6a and 6b). This substantial increased of radon concentration was clearly linked to the strong nocturnal inversion. Radon concentration in the morning did not show any changes with the sunrise, the decreasing of radon occurred after 10:00 with the dissipation of the nocturnal inversion. The mixing height during the night-time was less than 50 m a.g.l. and after broke up of the inversion reached the height 1430 m a.g.l. (Figure 4g).

In the summer months, compared with other seasons, the nocturnal inversions are rapidly dissolved because of the intense solar radiation (Kassomenos & Koletsis, 2005). In this case, the nocturnal inversion was broke-up within 5 hours after sunrise because of the latent heat flow, days before the high frequency of the precipitation occurred and the ground remained wet, a distinct part is converted into latent heat flow, due to evaporation, instead of sensible heat flow (Wezel & Chang, 1988). The daytime was followed with precipitation and radon concentration decreased on the typical mean level (Figures 4a and 4f).

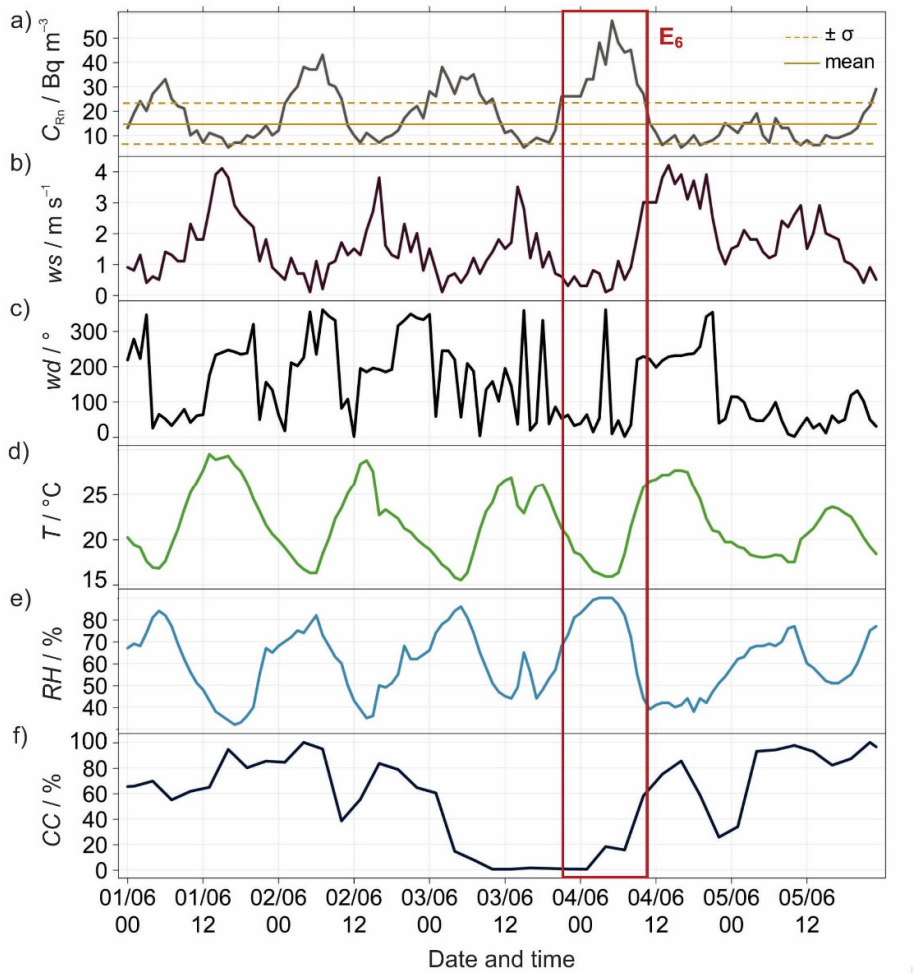

Fig. 6. Time series of a) atmospheric radon concentration (C_{Rn}), b) wind speed (*ws*), c) wind direction (*wd*), d) air temperature (*T*), e) relative humidity (*RH*) and f) cloud cover (*CC*) during the period before and after +σ E_6 (03/06/2017 21:00 – 04/06/2017 10:00).

3.2. *Changes on atmospheric radon as a function of the temporal variation of exhalation rate and wind direction/speed (E_4)*

Overcast conditions with a precipitation (~ 6 mm) occurred several days before the E_4 (Figures 3f and 7f). On 16 January after 12:00 the radon concentration decreased and did not show the variation for next 35 hours (Figure 7a). Since Ljubljana Basin has a lot of underground waters, the level of them might be increased because of the precipitation and affecting the exhalation rate. The soil moisture significantly reduces the diffusion and exhalation of radon from the soil (Nazaroff, 1992; Mattsson, 1970). By not neglecting the fact that air temperature before and during E_4 was under 0°C (Figure 7d), which could lead to the conclusion that the soil has been frozen and affected the total reduction of exhalation rate (Feichter & Crutzen, 1990; Jacob & Prather, 1990).

The decrease of the radon concentration during E_4 in Figure 7a was related to the change of the wind speed and direction (Figures 7b and 7c). The eastern katabatic wind coming from the Posavje hills (the highest peak 1219 m a.s.l.) with enhanced wind speed (Figure 8). Generally, the katabatic wind is nocturnal wind but it can also be formed in the daytime over snow- or ice-covered slopes (Figure 8) (Stull, 2011). Katabatic winds might lead to the formation of fog (Stull, 2011) in the Ljubljana Basin (Figure 7f).

Well-mixed conditions have occurred during the E_4 with mixing height more than 1000 m a.g.l. during daytime and as low as 500 m a.g.l. at night (Figure 3g).

3.3. *The effect of origin of air masses on atmospheric radon (E_7)*

Temporal variation of atmospheric radon, wind speed and direction, air temperature, relative humidity and cloud cover during the period before and after E_7 is shown in Figure 9 and the 4 days backward trajectories of air masses passing the measurement location in Ljubljana Basin are shown in Figure 10. A decreased of radon concentration after midnight on 7 June (Figure 9a) revealed the influence of maritime air masses originating over the Adriatic Sea and travelling with the southwestern moderate wind (Figure 11). After the E_7 the air masses were continental (Figure 10) and an increase of the radon concentration was observed on the typical mean level for the subsequent days (Figure 9a).

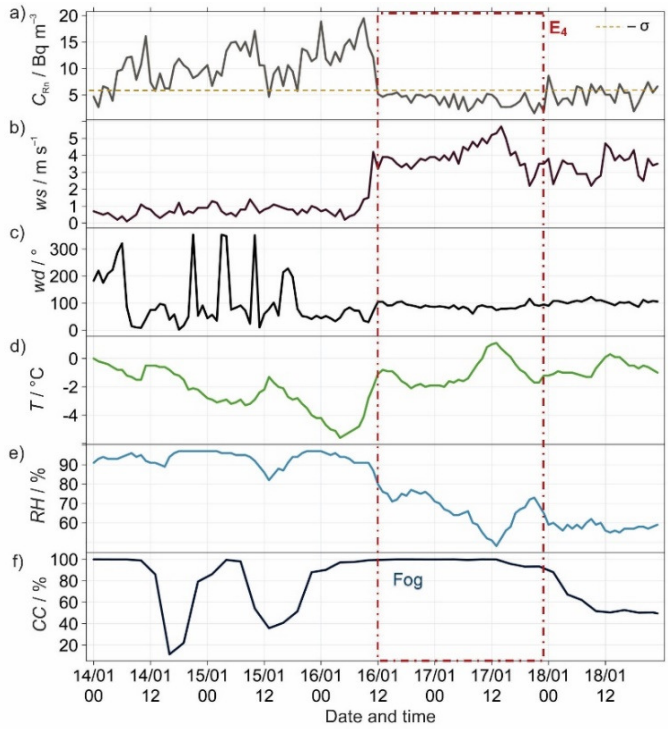

Fig. 7. Time series of a) atmospheric radon concentration (C_{Rn}), b) wind speed (*ws*), c) wind direction (*wd*), d) air temperature (*T*), e) relative humidity (*RH*) and f) cloud cover (*CC*) during the period before and after $-\sigma$ E_4 (16/01/2017 13:00 – 17/01/2017 23:00)

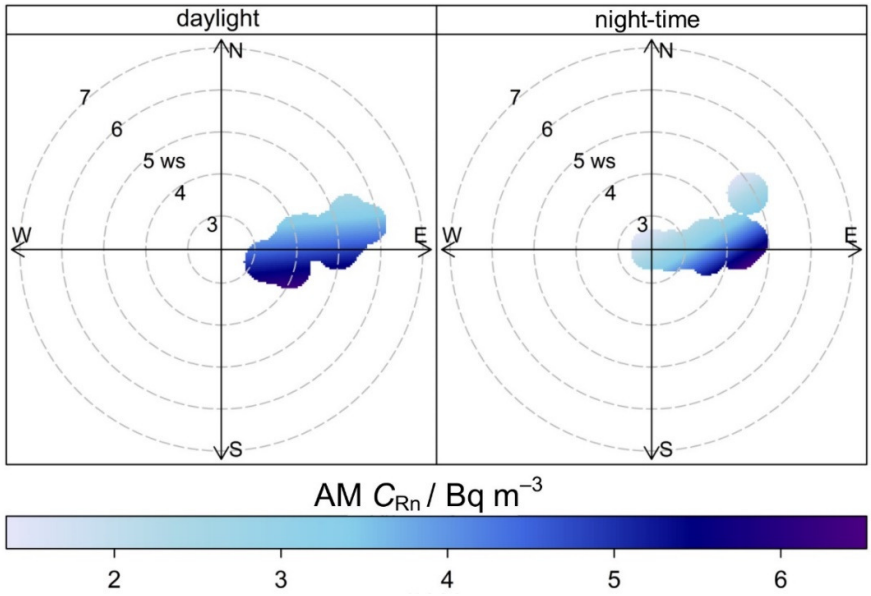

Fig. 8. The bivariate polar plot of mean atmospheric radon concentration on the day and night-time jointly with eastern (katabatic) wind during the $-\sigma$ E_4 (16.01.2017 13:00 – 17.01.2017 23:00).

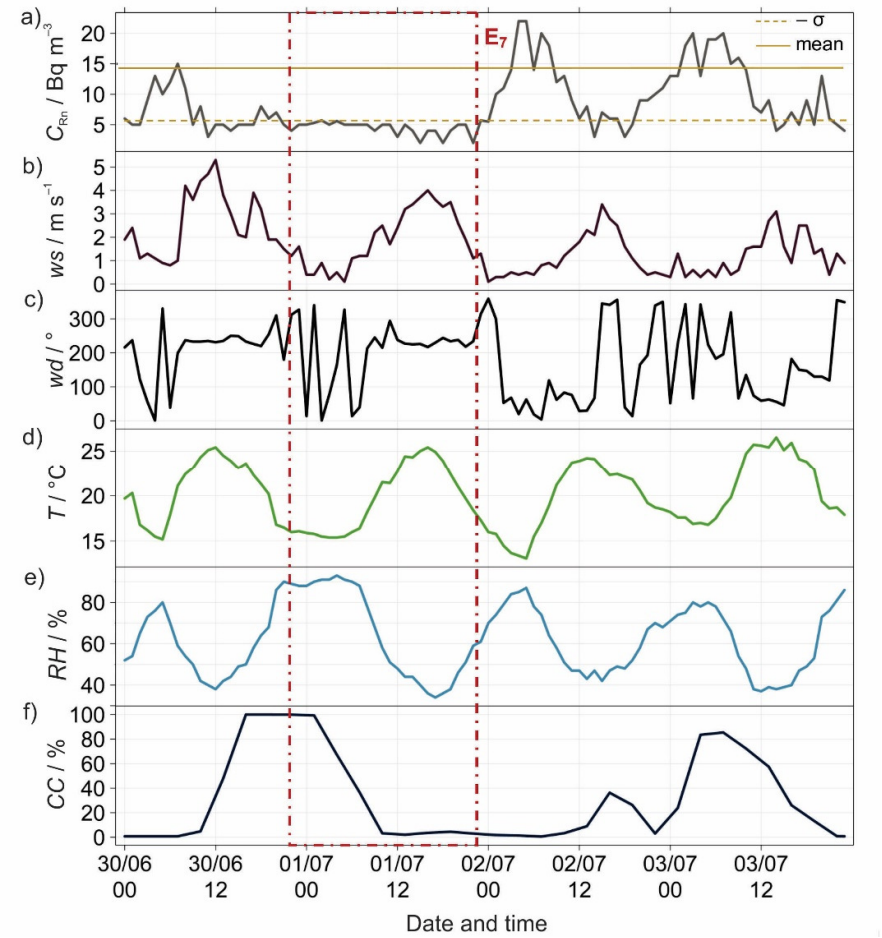

Fig. 9. Time series of a) atmospheric radon concentration (C_{Rn}), b) wind speed (*ws*), c) wind direction (*wd*), d) air temperature (*T*), e) relative humidity (*RH*) and f) cloud cover (*CC*) during the period before and after $-\sigma$ E_7 (01/07/2017 00:00 – 02/07/2017 00:00)

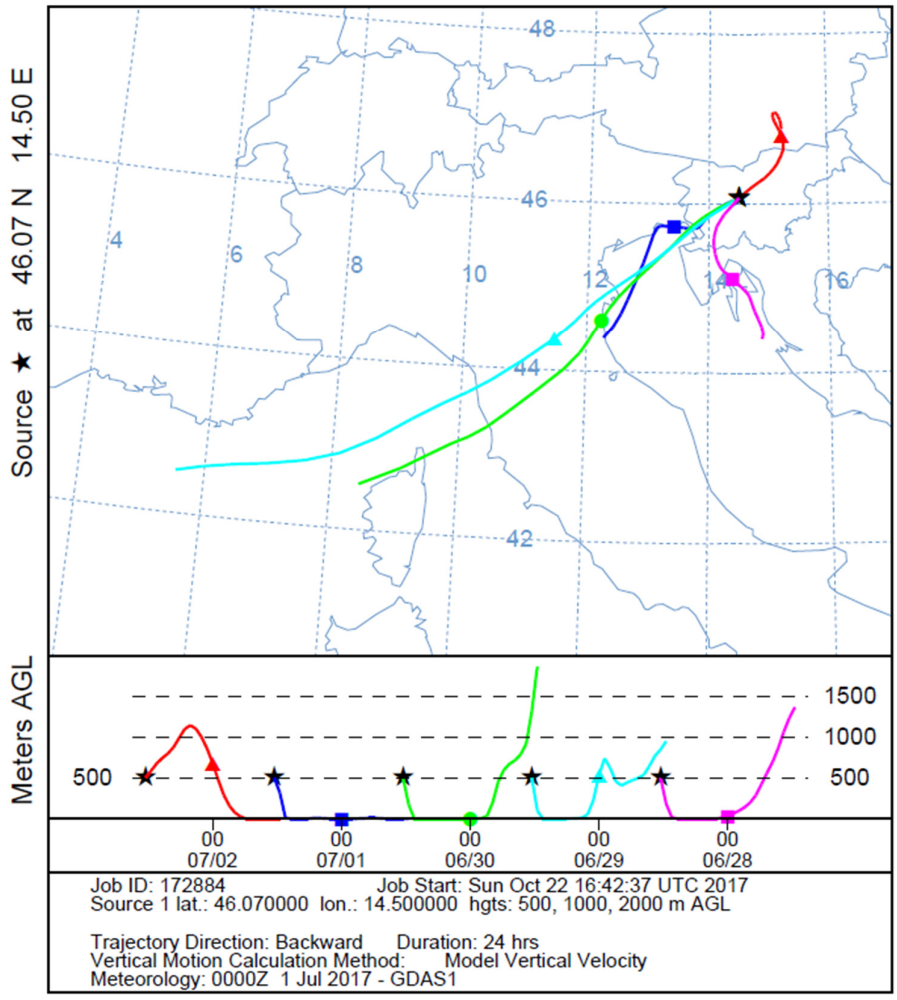

Figure 10. Four days HYSPLIT back trajectories centred on meteorological station Ljubljana Bežigrad for –σ E_7 (01/07/2017 00:00 – 02/07/2017 00:00), shown grouped for each day (every 24 hours new trajectory) and coloured accordingly

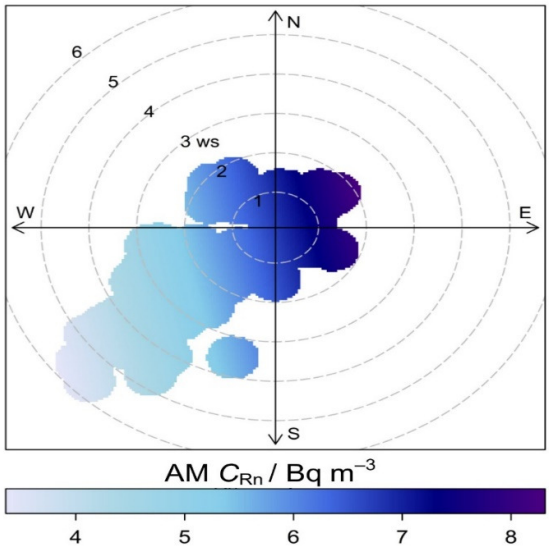

Figure 11. The bivariate polar plot of mean atmospheric radon concentration jointly with the southwestern wind during the *–σ E_7* (01/07/2017 00:00 – 02/07/2017 00:00)

4. CONCLUSIONS

The one year data series of atmospheric radon, obtained at the Ljubljana Bežigrad meteorological station during December 2016 – November 2017, was analyzed along with the meteorological data and back trajectory information.

Radon concentration exhibited the annual cycle with a higher mean in the winter (20.7 ± 15.5 Bq m^{-3}) and a lower mean in the summer (14.6 ± 9 Bq m^{-3}) reflecting the PBL evolution on a seasonal timescale. Most of the time, radon showed the typical diurnal variation following the related mean seasonal level attributed to the vertical mixing processes. Among this typical pattern, we were able to detect with a simple statistical analysis based on $\pm\sigma$ deviations of the atmospheric radon concentration from the seasonal mean value nine events (E_i). The parameter persistent/nocturnal inversion was the main reason for $+\sigma$ E_i. The temporal variation of the exhalation rate, wind direction/speed and maritime air masses have been recognized as responsible influencing parameter for $-\sigma$ E_i.

The obtained results imply that atmospheric radon is a suitable tool for studying the building and breaking up of the persistent/nocturnal inversion in the basin. The determining of the equivalent mixing height based on the radon box model is much simpler because there is no need to take into account the horizontal advection transport and residual radon concentration from a previous, deeper, mixed layer during the inversion periods. Radon proved to be a good indicator of the wind direction and influence of the origin of air masses.

The temporal variability of the exhalation rate of radon, which was mainly due to soil moisture, seems to influence the variation of the atmospheric radon. Therefore, the long-term experimental data of radon exhalation on the Ljubljana Basin would improve the usage of radon as an atmospheric tracer.

Acknowledgements: The authors acknowledge the financial support from the Slovenian Research Agency (research core funding No. P1-0143) and from the Public Scholarship, Development, Disability and Maintenance Fund of the Republic of Slovenia (Contract no. 11011-44/2016-18). The authors also gratefully acknowledge the Environmental Agency of the Republic of Slovenia for the permission provided to install the weather instrument shelter for radon monitoring on their land and for providing the meteorological data, NOAA Air Resources Laboratory (ARL) the using of the HYSPLIT transport and dispersion model, and the READY website (http.//www.arl.noaa.gov/ready.php).

REFERENCES

ARSO, Slovenian Environment Agency (Slovenian: Agencija Republike Slovenije za okolje): Climate characteristics of Ljubljana - Wind Rose for the City of Ljubljana (2017). http://meteo.arso.gov.si/uploads/probase/www/climate/table/sl/by_variable/wind/Ljubljana.html.

Burian I., & Otahal P. (2009): Radon and its decay products in outdoor air. *Applied Radiation and Isotopes*, **67** (5), 881–883.

Butterweck G., Reineking A., Kesten J., & Porstendörfer J. (1994): The use of the natural radioactive noble gases radon and thoron as tracers for the study of turbulent exchange in the atmospheric boundary layer—case study in and above a wheat field. *Atmospheric Environment*, **28** (12), 1963–1969.

Carslaw D. C., & Ropkins K. (2012): Openair – an R package for air quality data analysis. *Environmental Modelling & Software*, **27**, 52–61.

Chambers S. D., Williams A. G., Crawford J., & Griffiths A. D. (2015): On the use of radon for quantifying the effects of atmospheric stability on urban emissions. *Atmospheric Chemistry and Physics*, **15** (3), 1175–1190.

Chambers S., Williams A. G., Zahorowski W., Griffiths A., & Crawford J. (2011): Separating remote fetch and local mixing influences on vertical radon measurements in the lower atmosphere. *Tellus B*, **63** (5), 843–859.

Chambers S. D., Zahorowski W., Williams A. G., Crawford J., & Griffiths A. D. (2011): Identifying tropospheric baseline air masses at Mauna Loa Observatory between 2004 and 2010 using Radon-222 and back trajectories. *Journal of Geophysical Research: Atmospheres*, **118** (2), 992–1004.

Chen X., Paatero J., Kerminen V.-M., Riuttanen L., Hatakka J., Hiltunen V., Paasonen P., Hirsikko A., Franchin A., Manninen H. E., Petaja T., Viisanen Y., & Kulmala M. (2016): Responses of the atmospheric concentration of radon-222 to the vertical mixing and spatial transportation. *Boreal Environment Research,* **21**(3–4), 299–318.

Cohen L. D., Barr S., Krablin R., & Newstein H. (1972): Steady-state vertical turbulent diffusion of radon. *Journal of Geophysical Research*, **77**(15), 2654–2668.

Dörr H., Kromer B., Levin I., Münnich K. O., & Volpp H. J. (1983): CO_2 and Radon-222 as tracers for atmospheric transport. *Journal of Geophysical Research: Oceans*, **88** (C2), 1309–1313.

Etiope G., & Martinelli G. (2002): Migration of carrier and trace gases in the geosphere: an overview. *Physics of the Earth and Planetary Interiors*, **129** (3), 185–204.

Feichter J., & Crutzen P. J. (1990): Parameterization of vertical tracer transport due to deep cumulus convection in a global transport model and its evaluation with ^{222}Radon measurements. *Tellus B*, **42** (1), 100–117.

Fontan J., Guedalia D., Druilhet A., & Lopez A. (1979): Une methode de mesure de la stabilite verticale de l'atmosphere pres du sol. *Boundary-Layer Meteorology,* **17**, 3–14 (in French, with English abstract).

Gregorič A., Vaupotič J., Kardos R., Horváth M., Bujtor T., & Kovács T. (2013): Radon emanation of soils from different lithological units. *Carpathian Journal of Earth and Environmental Sciences*, **8** (2), 185–190.

Griffiths A. D., Parkes S. D., Chambers S. D., McCabe M. F., & Williams A. G. (2013): Improved mixing height monitoring through a combination of lidar and radon measurements. *Atmospheric Measurement Techniques*, **6** (2), 207–218.

Grossi C., Àgueda A., Vogel F. R., Vargas A., Zimnoch M., Wach P., Martín J. E., López-Coto I., Bolívar J. P., Morguí J. A., & Rodó X. (2016): Analysis of ground- based ^{222}Rn measurements over Spain: Filling the gap in southwestern Europe. *Journal of Geophysical Research: Atmospheres*, **121** (18) 11021–11037.

Jacob D. J., & Prather M. J. (1990): Radon-222 as a test of convective transport in a general circulation model. *Tellus B*, **42** (1), 118–134.

Kassomenos P. A., & Koletsis I. G. (2005): Seasonal variation of the temperature inversions over Athens, Greece. *International Journal of Climatology*, **25** (12), 1651–1663.

Largeron Y., & Staquet C. (2016): Persistent inversion dynamics and wintertime PM_{10} air pollution in Alpine valleys. *Atmospheric Environment*, **135**, 92–108.

Levin I., Born M., Cuntz M., Langendörfer U., Mantsch S., Naegler T., Schimdt M., Varlagin A., Verclas S., & Wagenbach D. (2002): Observations of atmospheric variability and soil exhalation rate of radon-222 at a Russian forest site. Technical approach and deployment for boundary layer studies. *Tellus B*, **54** (5), 462–475.

Levin I., Glatzel-Mattheier H., Marik T., Cuntz M., Schmidt M., & Worthy D. E. (1999): Verification of German methane emission inventories and their recent changes based on atmospheric observations. *Journal of Geophysical Research: Atmospheres*, **104** (D3), 3447–3456.

Mattsson R. (1970): Seasonal variation of short-lived radon progeny, Pb^{210} and Po^{210}, in ground level air in Finland. *Journal of Geophysical Research*, **75** (9), 1741–1744.

Mazur J., & Kozak K. (2014): Complementary system for long term measurements of radon exhalation rate from soil. *Review of Scientific Instruments*, **85** (2), 022104.

Moses H., Stehney, A. F. & Lucas H. F. (1960): The effect of meteorological variables upon the vertical and temporal distributions of atmospheric radon. *Journal of Geophysical Research*, **65** (4), 1223–1238.

Nazaroff W. W. (1992): Radon transport from soil to air. *Reviews of Geophysics*, **30** (2), 137–160.

Pak M. (1992): Ljubljana. In: Javornik M. (ed.), *Enciklopedija Slovenije 6*, 218–220. Mladinska knjiga, Ljubljana.

Pal S., Lopez M., Schmidt M., Ramonet M., Gibert F., Xueref-Remy I., & Ciais P. (2015): Investigation of the atmospheric boundary layer depth variability and its impact on the ^{222}Rn concentration at a rural site in France. *Journal of Geophysical Research: Atmospherees*, **120** (2), 623–643.

Papachristodoulou C., Ioannides K., & Spathis S. (2007): The effect of moisture content on radon diffusion through soil: assessment in laboratory and field experiments. *Health Physics*, **92** (3), 257–264.

R Core Team (2013): *R: A Language and Environment for Statistical Computing*. R Foundation for Statistical Computing, Vienna, Austria. http://www.R-project.org/.

Sesana L., Caprioli E., & Marcazzan G. M. (2003): Long period study of outdoor radon concentration in Milan and correlation between its temporal variations and dispersion properties of atmosphere. *Journal of Environmental Radioactivity*, **65** (2), 147–160.

Schnelle K. B., & Brown C. A. (2002): *The Air Pollution Control Technology Handbook*. CRC Press.

Stull R. (2011): *Meteorology for Scientists & Engineers,* 3rd Edition. University of British Columbia.

Šajn R., Gosar M., Bidovec M., Pirc S., & Alijagić J. (2011): Geochemical mapping of Ljubljana urban and suburban area, Slovenia. In: *Mapping the Chemical Environment of Urban Areas*, 375–392. John Wiley & Sons, New York.

Ussler W., Chanton J. P., Kelley C. A., & Martens C. S. (1994): Radon-222 tracing of soil and forest canopy trace gas exchange in an open canopy boreal forest. *Journal of Geophysical Research: Atmospheres*, **99** (D1), 1953–1963.

Van der Laan S., Van der Laan-Luijkx I. T., Zimmermann L., Conen F., & Leuenberger M. (2014): Net CO_2 surface emissions at Bern, Switzerland inferred from ambient observations of CO_2, $\delta(O_2/N_2)$, and ^{222}Rn using a customized radon tracer inversion. *Journal of Geophysical Research: Atmospheres*, **119** (3), 1580–1591.

Vaupotič J., Kobal I., & Križman M. J. (2010): Background outdoor radon levels in Slovenia. *Nukleonika*, **55**, 579–582.

Vinuesa J. F., Basu S., & Galmarini S. (2007): The diurnal evolution of ^{222}Rn and its progeny in the atmospheric boundary layer during the Wangara experiment. *Atmospheric Chemistry and Physics Discussions*, **7** (3), 8895–8931.

Vogel F. R., Ishizawa M., Chan E., Chan D., Hammer S., Levin I., & Worthy D. E. J. (2012): Regional non-CO_2 greenhouse gas fluxes inferred from atmospheric measurements in Ontario, Canada. *Journal of Integrative Environmental Sciences*, **9** (sup1), 41–55.

Wada A., Matsueda H., Murayama S., Taguchi S., Hirao S., Yamazawa H., Moriizumi J., Tsuboi K., Niwa Y, & Sawa Y. (2013): Quantification of emission estimates of CO_2, CH_4 and CO for East Asia derived from atmospheric radon-222 measurements over the western North Pacific. *Tellus B: Chemical and Physical Meteorology*, **65** (1), 1803–7.

Wetzel P. J., & Chang J. T. (1988): Evapotranspiration from nonuniform surfaces: A first approach for short-term numerical weather prediction. *Monthly Weather Review*, **116** (3), 600–621.

Whiteman C. D., Bian X., & Zhong S. (1999): Wintertime evolution of the temperature inversion in the Colorado Plateau Basin. *Journal of Applied Meteorology*, **38** (8), 1103–1117.

Whiteman C. D., Pospichal B., Eisenbach S., Weihs P., Clements C. B., Steinacker R., Mursch-Radlgruber E., & Dorninger M. (2004): Inversion breakup in small Rocky Mountain and Alpine basins. *Journal of Applied Meteorology*, **43** (8), 1069–1082.

Williams A. G., Zahorowski W., Chambers S., Griffiths A., Hacker J. M., Element A., & Werczynski S. (2011): The vertical distribution of radon in clear and cloudy daytime terrestrial boundary layers. *Journal of the Atmospheric Sciences*, **68** (1), 155–174.

World Health Organization: *WHO Handbook on Indoor Radon: A Public Health Perspective*. Geneva: World Health Organization, 2009.

Zahorowski W., Chambers S. D., & Henderson-Sellers A. (2004): Ground based radon-222 observations and their application to atmospheric studies. *Journal of Environmental Radioactivity*, **76** (1), 3–33.

Zahorowski W., Chambers S., Wang T., Kang C. H., Uno I., Poon S., Oh S. N., Werczynski S., Kim J., & Henderson-Sellers A. (2005): Radon-222 in boundary layer and free tropospheric continental outflow events at three ACE-Asia sites. *Tellus B*, **57** (2), 124–140.

Zhang K., Feichter J., Kazil J., Wan H., Zhuo W., Griffiths A. D., Sartorius H., Zahorowski W., Ramonet M., Schmidt M., Yver C., Neubert R. E. M., & Brunke E. G. (2011): Radon activity in the lower troposphere and its impact on ionization rate: a global estimate using different radon emissions. *Atmospheric Chemistry and Physics*, **11** (15), 7817–7838.

Р е з и м е

ПАРАМЕТРИ КОИ ВЛИЈААТ ВРЗ ОТСТАПУВАЊЕТО НА КОНЦЕНТРАЦИЈАТА НА РАДОН ОД НЕГОВАТА ТИПИЧНА ДНЕВНА ШЕМА ВО ЗИМСКА И ЛЕТНА СЕЗОНА

Дафина Кикај[1], Јања Ваупотич[2]

[1]Училиште за постдипломски студии Јожеф Штефан,
Јамова цеста 39, 1000 Љубљана, Словенија
[2]Институт Јожеф Штефан, Оддел за науки на животната средина,
Јамова цеста 39, 1000 Љубљана, Словенија
dafina.kikaj@ijs.si

Клучни зборови: атмосферски радон; континуирано мерење; девијации во концентрацијата; слој на планетарна граница; постојана инверзија; воздушни маси

Радонот (^{222}Rn) се користи како атмосферски трејсер за проучување на вертикалните процеси на мешање во рамките на планетарните слоеви (PBL). Поради тоа, временската серија часовни атмосферски концентрации на радон добиена во Љубљана беше анализирана заедно со метеоролошките податоци и информациите за соодветните траектории од декември 2016 до ноември 2017 година. Концентрацијата на радон покажала годишен циклус со највисока средна вредност во зима (20.7 ± 15.5 Bq m^{-3}) и најниска средна вредност во лето (14.6 ± 9 Bq m^{-3}) одразувајќи ја еволуцијата на PBL на ниво на сезонска временска скала. Во најголем дел од времето, радонот покажал карактеристични дневни варијации следејќи ги поврзаните средни сезонски нивоа, а што може да биде припишано на процесите на вертикално мешање. Меѓу овие типични шеми, девијациите на концентрацијата на атмосферскиот радон за повеќе од ±σ од соодветната сезонска средна вредност биле откриени во 9 случаи (±σ E_i) во зимска и летна сезона користејќи едноставна статистичка анализа. Параметарот перзистентна/ноќна инверзија обично е причина за +σ E_i, додека временската варијација на стапката на испарување, насоката на ветерот/брзината на ветерот и поморските воздушни маси се параметрите одговорни за –σ E_i.